Geofísica Internacional (2026) **65-1**: 1951- 1965

High chlorophyll-a concentration events related to vertical stratification variability during the dry season in the Western Margin of the Gulf of Tehuantepec

A. Cristóbal Reyes-Hernández[1]*, Andrés López-Pérez[3], Miguel A. Ahumada-Sempoal[1], Pedro Cervantes-Hernández[1] and María del Carmen Alejo Plata[2]

Abstract

Five high chlorophyll-a concentration events, > 2.3 mg m^{-3}, developed from December 2011 to March 2012, are analyzed in the context of the observed vertical stratification variability created by the interaction of wind and the coastal mesoscale circulation at La Boquilla, a point in the Western Margin of the Gulf of Tehuantepec. The analysis is based on records of temperature at 5 and 24 m depth, water velocity profiles, wind velocity at a nearby meteorological station, Level 3 MODIS-Aqua daily chlorophyll-a concentration, and daily ASCAT winds. Most of the high chlorophyll-a concentration events occurred when mesoscale cyclonic circulation was close to La Boquilla, under westerly wind stress $\tau > 0.02\,N\,m^{-2}$. Each high chlorophyll-a event succeeded the dissipation of a thermal front and the development of a two-layer exchange between the western margin and the central gulf. The highest chl-a concentration occurred when upwelling and mixing modified the stratification. The modest high chl-a concentration occurred when mixing alone modified the stratification.

Key words: High chlorophyll-a concentration; stratification, upwelling, and mixing; westerly wind and mesoscale oceanic circulation; satellite and coastal observations; Eastern Tropical Pacific.

Resumen

Cinco episodios con alta concentración de clorofila-a, >2.3 mg m^{-3}, ocurridos de diciembre del 2011 a marzo del 2012, son analizados en el contexto de la variabilidad en la estratificación vertical creada por la interacción entre el viento y la circulación costera de mesoescala en La Boquilla, un punto en el Margen Occidental del Golfo de Tehuantepec. El análisis utiliza registros de temperatura a 5 y 24 m de profundidad, perfiles de velocidad del agua, velocidad del viento en una estación meteorológica cercana, datos diarios de concentración de clorofila-a, nivel 3 de MODIS-Aqua y de vientos ASCAT. La mayoría de los eventos con alta concentración de clorofila-a ocurrieron cuando la circulación de mesoescala cercana a La Boquilla fue ciclónica y el esfuerzo del viento $\tau > 0.02$ N m^{-2}. Cada evento con alta concentración de clorofila-a siguió a la disipación de un frente térmico y la formación de un flujo de dos capas entre el margen occidental y el golfo central. Las concentraciones de clorofila-a más altas ocurrieron cuando la surgencia y la mezcla modificaron la estratificación. Las altas concentraciones de clorofila más modestas, ocurrieron cuando sólo la mezcla modificó la estratificación.

Palabras clave: alta concentración de clorofila-a, estratificación, surgencia y mezcla, viento del oeste y circulación oceánica de mesoescala, observaciones costeras y satelitales, Pacífico Tropical Oriental.

Received: September 9, 2024; Accepted: October 9, 2025; Published on-line: January 1, 2026.

Editorial responsibility: Dr. Joel Rosales-Rodríguez

* Corresponding author: A. Cristóbal Reyes-Hernández, creyes@angel.umar.mx
[1] Universidad del Mar, Instituto de Recursos, Puerto Ángel, Oaxaca, México.
[2] Universidad del Mar, Laboratorio de Histología, Instituto de Recursos, Puerto Ángel, Oaxaca, México.
[3] Universidad Autónoma Metropolitana Unidad Iztapalapa, Laboratorio de Arrecifes y Biodiversidad (ARBIOLAB)/Laboratorio de Ecosistemas Costeros, Departamento de Hidrobiología, Ciudad de México, México.

A. Cristóbal Reyes-Hernández, Andrés López-Pérez, Miguel A. Ahumada-Sempoal, Pedro Cervantes-Hernández, María del Carmen Alejo Plata
https://doi.org/10.22201/igeof.2954436xe.2026.65.1.1823

1. Introduction

1.1 Motivation

High chlorophyll-a concentration episodes occur after turbulent mixing in the water column redistributes the nutrients trapped in the thermocline upwards, and water transparency allows sufficient light for photosynthesis (Mann and Lazier, 1991). From a physical point of view, the chlorophyll concentration [chl-a] reached is highly dependent on stratification, upwelling, and mixing in the water column. Stratification maintains differences between layers, and mixing keeps vertical uniformity. Net surface heat flux gains, freshwater inputs, and subsurface flows lead to stratification; tidal currents and winds lead to mixing.

In the four Eastern Boundary Current Systems (EBCS) of the world, the upwelled water characteristics are highly dependent on the large-scale circulation patterns (Carr and Kearns, 2003). In particular, during the coastal upwelling season, along the Baja California coast, high [chl-a] episodes (averaging up to 5 mg m^{-3}) are dependent on the water characteristics carried by the California Current (Gaxiola-Castro *et al.* 2010). In the northern hemisphere, coastal upwelling results from the offshore Ekman transport in response to wind blowing parallel to a coast located to the left of the downwind stream. In contrast to the main EBCS, in the Gulf of Tehuantepec (GT), high [chl-a] episodes at the end of boreal winter have been related to the vigorous northerly wind events that blow offshore, perpendicular to the coast of Salina Cruz (SC; Blackburn, 1962; Lluch-Cota *et al.* 1997, Pennington *et al.* 2006). Near the coast, stirring through the water column seems to be the dominant mixing mechanism; offshore, the vertical Ekman pumping leads to upwelling, entrainment, and mixing (Blackburn, 1962; Trasviña *et al.*, 1995; Trasviña and Barton, 1997; Willet *et al.*, 2006). Under northerly wind events, high and low [chl-a] are expected to occur to the east and west of the wind jet, as a function of the respective wind-driven lifting and sinking of the thermocline (Pennington *et al.* 2006); however, the often observed high [chl-a] on the western margin of the Gulf of Tehuantepec (WMGT) and further west, after those in the central gulf, contrast with that picture. In a paper that is the precedent of this work, Reyes-Hernández and Ahumada-Sempoal (2022) noticed that, during the dry season, a frequent wind scenario in the GT consists of northerly winds over the central gulf and westerly winds over its western margin. When northerly winds relax, westerly winds can become dominant over the entire gulf, weakening stratification in the water column. In such a scenario, high [chl-a] peaks occur first in the central gulf and progress later towards the WMGT, where they should be related to coastal upwelling and mixing due to westerly, not to northerly winds (see, for example, Almaraz-Ruiz, 2013; Chapa-Balcorta *et al.*, 2015). Northerly winds over the gulf and westerly winds over its western margin occur so close in space and in time that their differentiated individual effect on high [chl-a] has been overlooked and credited only to northerly wind events (Blackburn, 1962; Lluch-Cota *et al.*, 1997; Pennington *et al.*, 2006). In comparison to the Baja California coast and the tropical Pacific coast of Mexico, in the Gulf of Tehuantepec, the average high [chl-a] from bottle collection is low: 0.33 mg m^{-3}, and it is also low compared to its SeaWIFS average estimations (0.89 mg m^{-3}; Pennington *et al.* 2006). Reyes-Hernández and Ahumada-Sempoal (2022) pointed out that the northerly wind on the GT creates a thermal front between its central and western waters. As the northerly wind relaxes, so does the thermal front, and an estuarine type of circulation between the central gulf and its western margin may initiate, with surface warm water flowing eastward and subsurface cool water flowing westward, increasing stratification in the WMGT.

The Pacific coast of Mexico and, in particular, the coast of the GT frequently harbors mesoscale eddies that originate in the Gulf itself or on the coast of Central America (Trasviña *et al.*, 1995; Zamudio *et al.*, 2006; Willet *et al.*, 2006; Reyes-Hernández *et al.*, 2016). In La Boquilla (LB), the effectiveness of the wind vertical mixing seems to result from the transit of mesoscale eddies throughout the area: Westerly wind and cyclonic circulation lead to an adequate vertical mixing between surface and subsurface waters; westerly wind and anticyclonic circulation lead to modest mixing (Reyes-Hernández and Ahumada-Sempoal, 2022, their Figure 8). It is expected that the variability in [chl-a] reflects the vertical stratification variability created by the interaction of wind and mesoscale eddies. In this work, we analyze the episodes in the WMGT where the surface [chl-a] matched or surpassed the whole time series average value (2.3 mg m^{-3}), from December 2011 to March 2012, concerning the observed thermal structure (stratification) and velocity field of the water column measured at LB. The objective is to explore how the high [chl-a] is related to the stratification variability in the WMGT, given by the wind and the mesoscale circulation.

1.2 Study site

The study site (Figure 1) is the same as given in Reyes-Hernández and Ahumada-Sempoal (2022); here we repeat some of the main features: The WMGT, on the coast of Oaxaca, southern Mexico, is part of a smooth cape that separates the Gulf of Tehuantepec from the western Mexican Pacific or the tropical Pacific off Central Mexico (Portela *et al.*, 2016). To facilitate our description, we term the western coast of this cape as the West Coast (Figure 1). The cape possesses a relatively high orography but a narrow coastal shelf reaching a depth beyond 200 m in less than 2 km from the coastline. The mooring site in the WMGT, located in LB, a small bay at about 15.67ºN and

96.46ºW, that is grossly oriented in an SW-NE direction, and is relatively close to a more than 100 m depth depression to the south. The average monthly [chl-a] values (1997-1998) for the GT are maxima from December to January (~ 0.51 mg m^{-3}), and minima in June (~ 0.17 mg m^{-3}; Cervantes-Hernández *et al.*, 2008), closely in phase with the strong northerly and weak southwesterly wind velocities in the western margin of the gulf (Reyes-Hernandez *et al.*, 2019).

2. Method

2.1 In situ measurements

In the mooring site, temperature and current data were gathered employing an ADCP SONTEK 250 kHz, a Microcat SB37-SMP probe, and a HOBO Data Logger UA-002-64, from December 16, 2011, to March 23, 2012. The depth of the mooring was 25 m, and measurements were performed at 5 m depth by the HOBO temperature logger and at 24 m depth by the ADCP and the Microcat SB37. Here we use the SB37 data. Temperature accuracies in the HOBO and SB37 are ±0.53°C and ±0.002°C, respectively. The temperature data from all the instruments were set to a temperature reference in the laboratory. Wind velocity was recorded using a meteorological station (MS) Davis, Vantage Pro2, located at Universidad del Mar in PA, 11 m above the ground, 78 m above sea level, approximately 380 m from the sea, and 4.1 km from the mooring site. The wind and speed accuracies are ±3° and ±5% of the measured speed. The ADCP pointed upwards, and the velocity profile consisted of 13 bins of 2 m size each. The horizontal and vertical components of the current velocity correspond to a Cartesian system positively oriented towards the East, North, and Upward. The accuracy of velocity, horizontal and vertical, is ±1.0% of the measured velocity or ±0.5 cm/s (SONTEK 250 kHz specifications). The configuration of the profiler is given in **Appendix A**. The sampling time interval was set to 30 minutes for all instruments. In this work, we employ the resulting hourly time series, smoothed with a 25-hour boxcar average. From now on, the temperatures at 5 and 24 meters depth are designated as T_{w5} and T_{w24}, respectively.

2.2 Synoptic data

Daily SST and Chlorophyll-a, level 3, images from NASA Ocean color (Goddard Space Flight Center, Ocean Biology Processing Group, 2014 **https://oceancolor.gsfc.nasa.gov/l3/**)

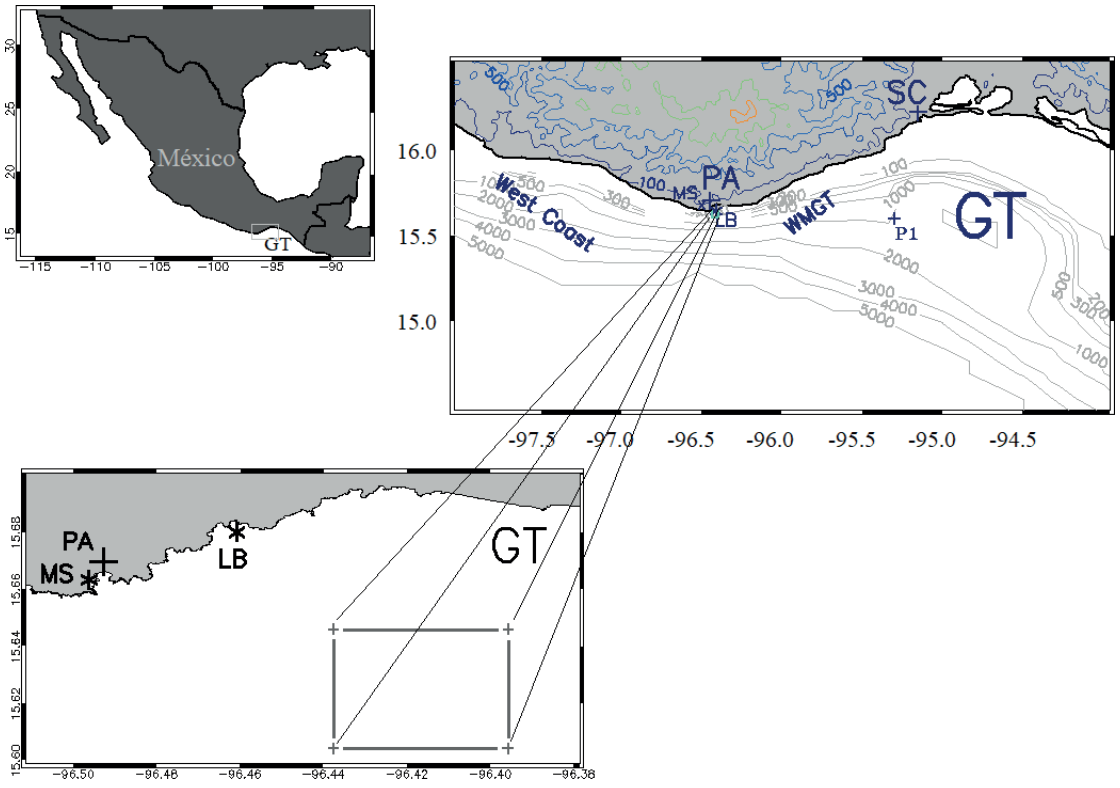

Figure 1. Location map. Gulf of Tehuantepec (GT); Puerto Ángel (PA); Salina Cruz (SC); Meteorological land-based station (MS); La Boquilla mooring site (LB). Orography (color lines) and bathymetry (grey lines) are in meters. The inlet shows the vertices in the green square corresponding to the four points used to calculate the average [chl-a] nearest to the LB mooring.

with a horizontal resolution of 4 km, were employed to construct daily composite images using a 3-day running average. A chlorophyll-a concentration time series was constructed by averaging the [chl_a] from the 4 points nearest to the LB mooring site: (-96.4375°, 15.6458°), (-96.4375°, 15.6042°), (-96.3958°, 15.6458°), and (-96.3958°, 15.6042°), to compare it to absolute dynamic topography (adt), stratification, wind, and current time series. The synoptic meteorological and oceanographic conditions in the GT along the period of observations consist of daily, level 3, surface ASCAT winds (**https://manati.star.nesdis.noaa.gov/datasets/ASCATData.php**) and AVISO daily, level 4, adt and geostrophic currents (**https://cds.climate.copernicus.eu/cdsapp#!/dataset/satellite-sea-level-global)**. The adt time series consists of a 2-point spatially averaged value immediately to LB (15.625000°N,-96.619995°W and 15.375000°N,-96.369995°W) from the adt maps (see Reyes-Hernandez et al, 2022). Because of the existence of remarkable [chl-a], spatial contrasts in the corresponding maps to shown ahead, the concentration is given as its logarithm base 10.

2.3 Procedure

The daily [chl-a] for LB was compared to the hourly stratification, wind stress, and current velocity profiles time series, within the synoptic adt, geostrophic currents, ASCAT wind, and [chl-a] maps. High [chl-a] is defined as that daily value superior to the time series temporal mean. We make use of the results of the spectral analysis applied to the stratification and wind time series by Reyes-Hernández and Ahumada-Sempoal (2022), where each hourly time series was smoothed by performing a 25-hour boxcar average to reduce diurnal fluctuations.

Stratification is defined as the observed vertical temperature difference between T_{w5} and T_{w24}, respectively. Reyes-Hernandez *et al.* (2022) concluded that tidal currents are not important in this site. For this reason, we assume that the wind is the main source of turbulent kinetic energy available for mixing. Also, the rate at which stratification decays is proportional to the wind stress Niiler and Kraus, 1977), $\tau = \rho_a C_D W_{10} \mid W_{10} \mid$, where ρ_a is the air density, W_{10} is the wind speed at 10 m above the sea level in neutral stability conditions, and CD is the wind speed-dependent drag coefficient as given in Large and Pond (1981). We use the qualitative evolution of T_{w5} and T_{w24} to infer the mechanisms strengthening or weakening the stratification. Mixing is identified when the upper and lower layers experience a respective temperature descent and ascent. Although the HOBO temperature uncertainty makes irrelevant any temperature difference less than 0.53°C, complete mixing is considered to occur when the difference decreases to 1.3 °C or less. Upwelling is identified when the temperature of the upper layer decreases while the deeper layer remains unchanged.

3. Results

3.1 Mesoscale activity, sea level, and velocity at LB

Between December 16, 2011, and March 22, 2012, the West Coast and the WMGT were subject to the transit of anticyclonic and cyclonic structures. Figure 2 shows the adt and geostrophic velocity maps throughout this period of time. From December 16, 2011, to January 2, 2012, an anticyclonic circulation approached LB, where it remained there up to January 5, when it started to withdraw southwestward. On January 22, the feature apparently had no influence on the circulation at LB; instead, geostrophic cyclonic circulation occupied the area. The anticyclone approached again to LB, just interrupted by a short receding from Feb 12 to 18, reaching its closest approximation to LB on Mar 4. Almost immediately, the anticyclone receded southwestward, except from Mar 11 to 14, when it moved to LB, and continued withdrawing after Mar 22, when cyclonic circulation approached LB.

The spatially averaged ADT time series of two points immediately to LB (Figure 3a; see section 2.2) exhibits each of the sea level fluctuations corresponding to this description. When compared to the actual residual (detided) sea level measured at LB, a general similarity is observed between the two records; however, the residual sea level is delayed by about 13 days and contains a shorter variability superimposed. Reyes-Hernandez and Ahumada-Sempoal (2022) noted that the residual sea level varied in correspondence with the wind and currents in the upper ten meters of depth.

Consistent with the anticyclonic and cyclonic approaches to LB, the spatially averaged geostrophic velocity direction turned anti-clockwise and clockwise, respectively (Figure 3b). At the LB mooring, the residual horizontal velocity direction recorded at 5.5 and 11.5 m depth also turned in a similar way; however, the direction at 5.5 m depth was noisier than at 11.5 m. As with the residual sea level, the residual velocity direction exhibited a delay relative to the geostrophic velocity direction. Anticlockwise delay was shorter at 5.5 m than at 11.5 m, but an opposite delay for each depth occurred for clockwise turning (Table 1).

3.2 Wind

In general, the anticyclonic and cyclonic circulations approaching to LB occurred, the former, in correspondence with northerly wind over the GT, and moderate and direction variable wind over the west coast (Figure 4; Jan 2, Feb 12, Mar 3 to 14), and the last one, in correspondence with westerly wind over both, the west coast and the GT (Jan 22, Feb 18, Mar 23 in replace of Mar 22). From Jan 23 to Mar 16, the anticyclonic circulation remained close to LB despite the westerly wind conditions present

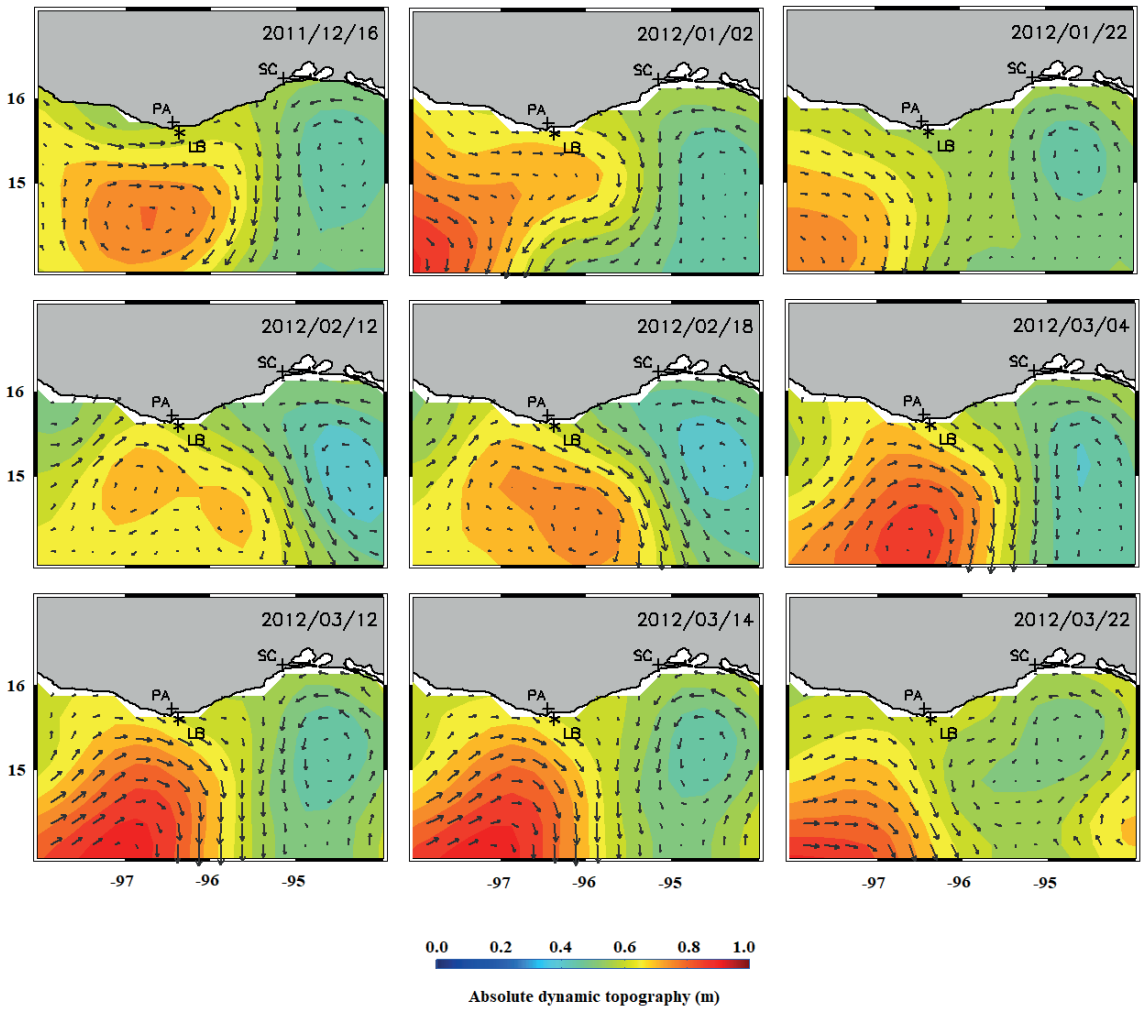

Figure 2. Absolute dynamic topography (adt) contours and geostrophic velocity (arrows). Dec 16, 2011; Jan 2, 22; Feb 12, 18; and Mar 4, 12, 14, and 22.

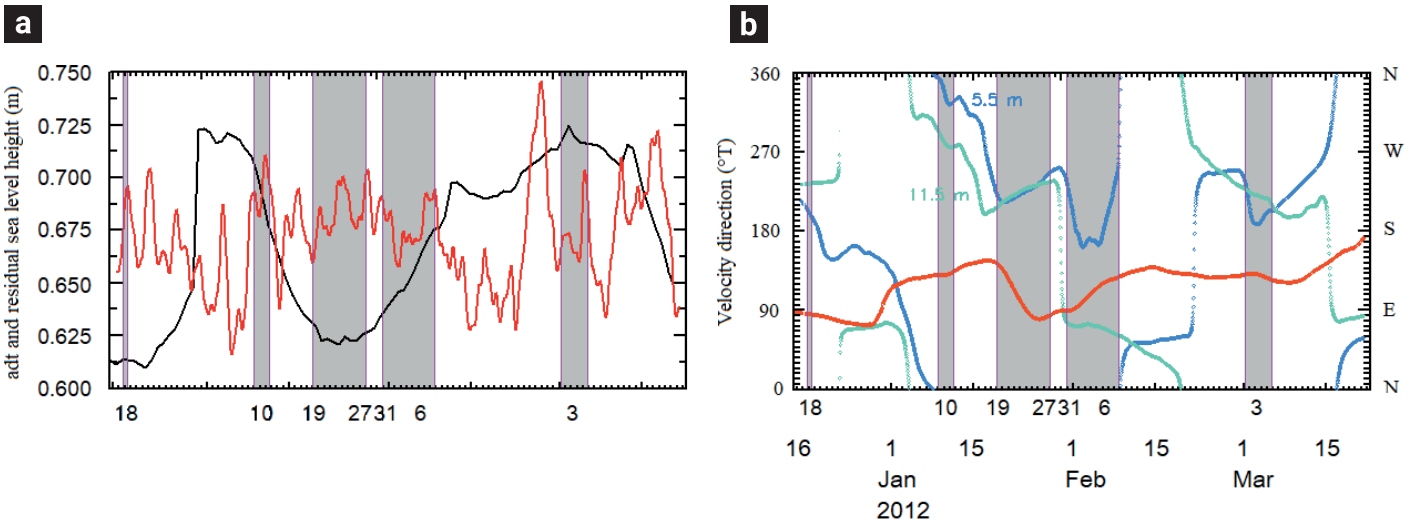

Figure 3. a) Spatially averaged adt time series (black line) and residual sea level height observed at LB plus the mean of adt (red line); b) velocity direction of the spatially averaged geostrophic velocity (red line) and residual velocity direction observed at 5.5 (blue line) and at 11.5 m depth (green line).

Table 1. Dates for anti-clockwise and clockwise velocity direction turning as estimated from the spatially averaged geostrophic velocity and as measured at the LB mooring at 5.5 and 11.5 meters depth.

Anti-clockwise			Clockwise		
geostrophic	**5.5 m**	**11.5 m**	**geostrophic**	**5.5 m**	**11.5 m**
Dec 16-28, 2011	Dec 16, 2011- Jan 20, 2012	Dec 31, 2011-Jan 17, 2012	Dec 28, 2011-Jan 17, 2012	Jan 20-30, 2012	Dec 16, 2011-Jan 31, 2012
Jan 17-27, 2012	Jan 30-Feb 3, 2012	Jan 29-Mar 10, 2012	Jan 26-Feb 14, 2012	Feb 3-Mar 1, 2012	Jan 17-29, 2012
Feb 15 to Mar 10, 2012	Mar 1 to 3, 2012	-----	Mar 10 to 22, 2012	Mar 4 to 22, 2012	Mar 10 to 16, 2012

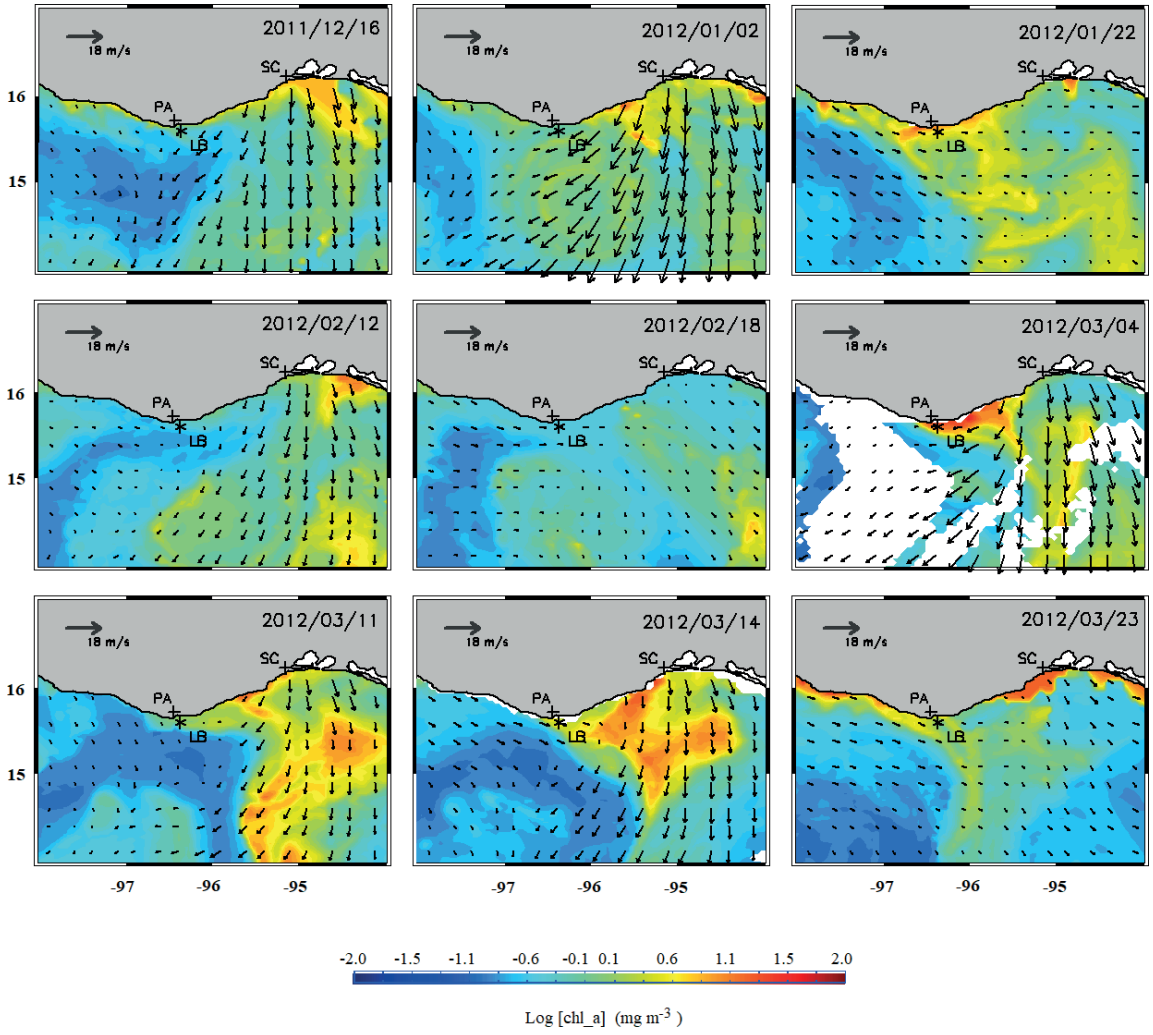

Figure 4. Wind conditions (arrows) and chlorophyll-a concentration contours. Dec 16, 2011; Jan 2, 22; Feb 12 and 18; and Mar 4, 12, 14, and 22.

on Feb 14-18, Feb 22, and Feb 29-Mar 2, which only produced small fluctuations in the adt time series (Figure 3a).

It is possible to claim that the residual sea level height and velocity direction observed at the LB mooring varied in general accordingly to the mesoscale circulation approaching the area. The two periods with anticyclonic circulation close to LB were in correspondence with strong northerly wind events over the GT. As the northerly winds decayed and westerly winds progressed towards the gulf, the anticyclonic circulation drifted southwestward, and cyclonic circulation occupied the LB mooring area.

3.3 Chlorophyll-a maxima events

The maps in Figure 4 also show the chlorophyll concentration [chl-a] related to the wind conditions. Under northerly wind on the GT, high [chl-a] was present at the central and eastern gulf

(Dec, 16, Jan 2, Feb 12, and Mar 11). Under westerly wind, high [chl-a] appeared at the WMGT and the west coast (Jan 22, Feb 18, and Mar 23). Mar 14 exhibited a mix of northerly and westerly wind conditions and [chl-a] distribution. The Mar 11 map is presented instead of the Mar 12 map, because of the large amount of missing [chl-a] pixels in the last one.

The correspondence between high [chl-a] at the WMGT and the west coast, and westerly wind is illustrated by the comparison between the spatially averaged [chl-a] daily time series near to the LB mooring site (see Section 2.2) and the westerly wind stress as measured at the MS (Figure 5a). Most of the [chl-a] values in the time series were below its mean, 2.3 mg m^{-3}, in contrast, the high [chl-a] events occurred under high westerly wind stress ($\tau > 0.02$ N m^{-2}), except from Jan 30-Feb 6.

3.4 Stratification and mixing

The high [chl-a] events occurred before full vertical mixing ($\Delta T \leq 1.3$ °C; Figure 5b), and were preceded by strong stratification ($\Delta T \sim 4$°C; Table 2), except on Dec 18.

Reyes-Hernández and Ahumada-Sempoal (2022) concluded that strong stratification and complete mixing occur under anticyclonic and cyclonic mesoscale circulation, respectively. They used the Bulk Richardson number (their Figure 8) to support their assertion, implying that mixing by westerly wind drag over the coastal edge of an anticyclone must be less effective than westerly wind drag over the coastal edge of a cyclone. They, however, did not attempt to discuss the mixing mechanisms involved. According to their findings, stratification varied at

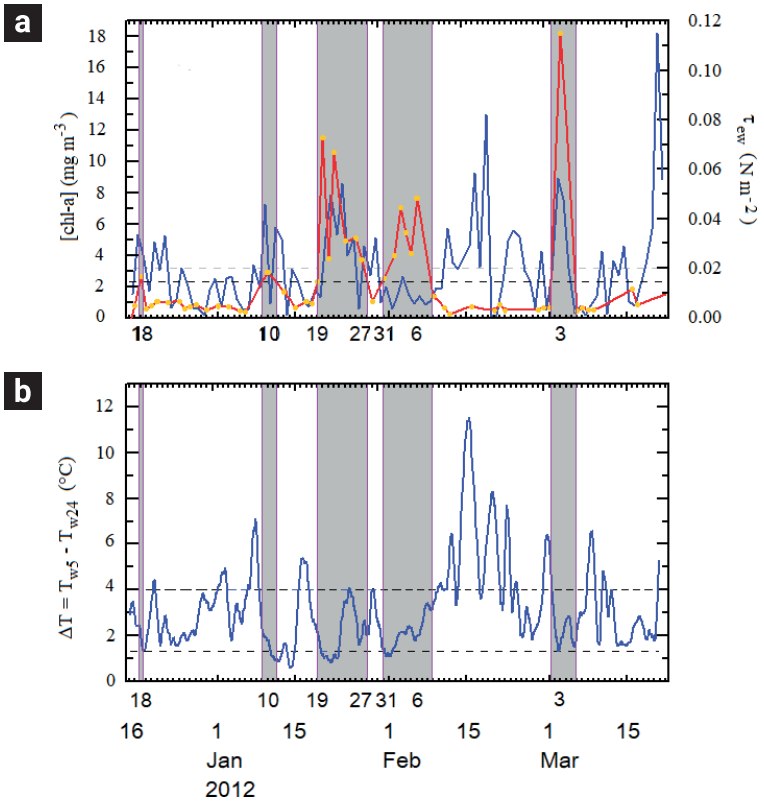

Figure 5. a) Spatially averaged chlorophyll-a concentration (red line) and westerly wind stress magnitude as measured at the MS (blue line). The dashed black line corresponds to the temporal mean 2.3 mg m^{-3} chl-a concentration. The gray dashed line corresponds to $|\tau| = 0.02$ N m^{-2}; b) Stratification. The lower and upper dashed lines correspond to 1.7 and 4 °C. The bars correspond to the high [chl-a] events.

Table 2. Dates for daily chlorophyll-a concentration maxima dates ([chl-a] ≥ 2.3 mg m^{-3}), complete mixing ($\Delta T \leq 1.3$ °C), and maximum stratification ($\Delta T \geq 4$ °C).

[chl-a] ≥ 2.3 mg m^{-3}	2011 Dec 18	2012 Jan 10	2012 Jan 19-27	2012 Jan 31- Feb 6	2012 Mar 3
$\Delta T \leq 1.3$°C	Dec18	Jan 10-14	Jan 19-22	Jan 30- Feb 2	Mar 3
$\Delta T \geq 4$°C	---	Jan 7-8	Jan 16	Jan 30	Feb 29-Mar 1

53 and 8 days, consistent with the mesoscale circulation and westerly wind speed variabilities, respectively.

Northerly winds over the GT demark the limits between the anticyclonic and cyclonic circulation between the West Coast and the GT, and create thermal fronts oriented, mainly, in a north-south direction. Cool vertically mixed water in the central gulf and warm surface water in the western side (Figure 6; Dec 16, Jan 2, Feb 12, Mar 4, Mar 12, and Mar 14). The location of the thermal front is in correspondence with the wind and mesoscale circulation. As the northerly wind relaxes, the front moves and dissipates. Although we did not perform an analysis, it seems that for relatively moderate northerly winds, anticyclonic or cyclonic circulation occupies the WMGT position, the front eastwards or westwards of LB, respectively. Also, strong northerly winds position the front westward of LB.

Figure 7 shows the surface horizontal temperature gradient between LB and P1, a point in the central gulf (Figure 1); its magnitude drops to a minimum generally in consistency with the northerly wind relaxation (Figure 7 upper panel; Dec 18-21; Jan 2-10; Jan 15-22; Jan 29-Feb 15; Feb 26-Mar 2), and compared to Fig, 5a, previous to westerly wind intensification and high [chl-a]. In this exercise, the weakening of the horizontal temperature gradient also appears when, under strong northerly wind on the GT, the thermal front is located to the west of LB; however, the weakening of the horizontal temperature gradient in response to the northerly wind relaxation is still valid. It will be seen that such was the case from Jan 19 to 27 and from Jan 30 to Feb 6, 2012.

Consistent with the weakening of the density gradient, a mainly east-west two-layer flow occurs at about the top 12 m in the LB mooring. Surface warm layer flows from the west to the central gulf, and a subsurface mixed, cool layer flows in the opposite direction (Figure 7, lower panel). The lower layer flow should increase the vertical thermal stratification at LB, working as a source of nutrients and chlorophyll. The posterior mixing

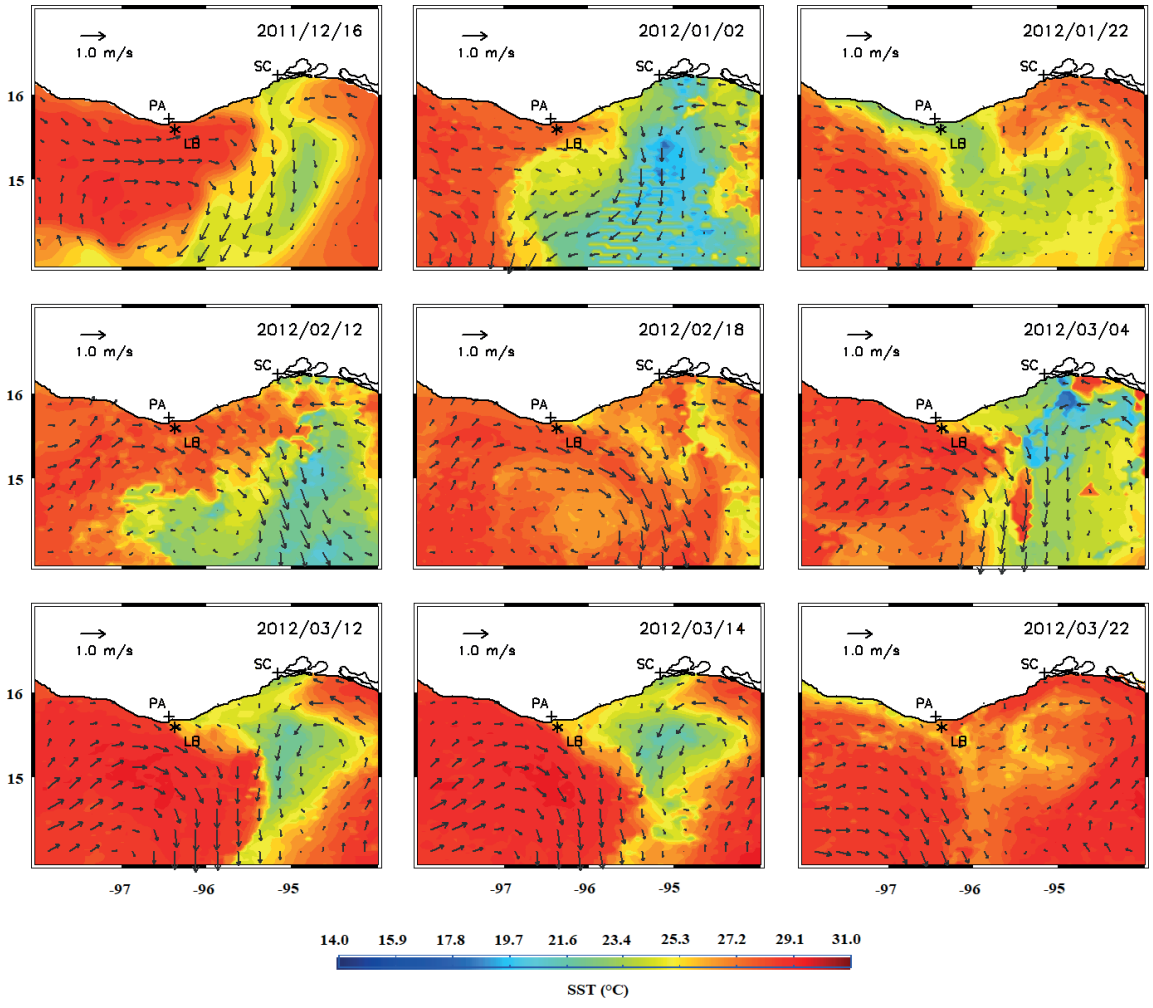

Figure 6. SST contours and corresponding adt geostrophic velocity vectors. Dec 16, 2011; Jan 2, 22; Feb 12, 18; and Mar 4, 12, 14, and 22.

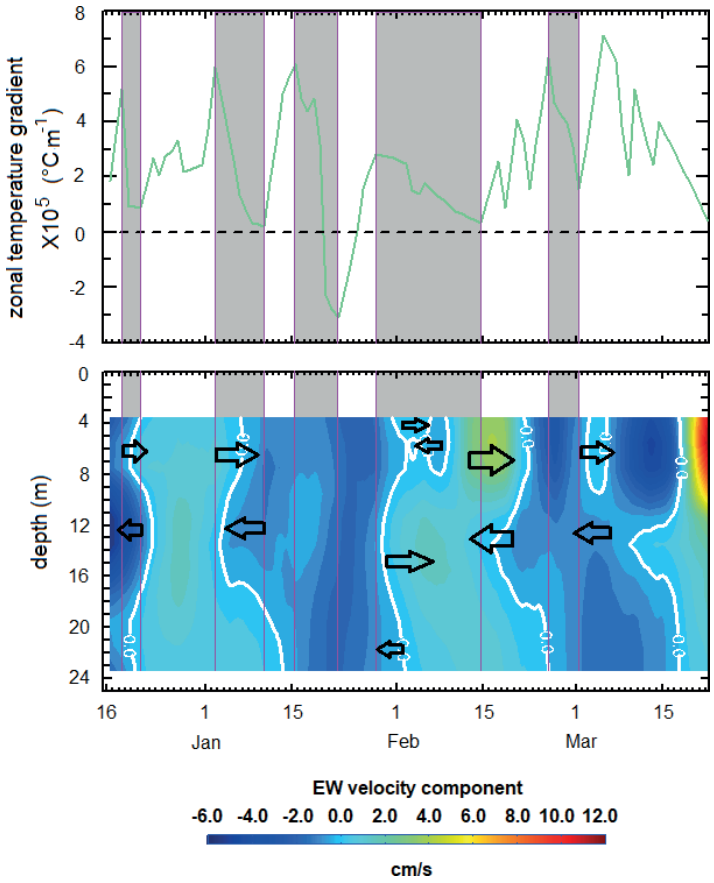

Figure 7. Temperature gradient $\times 10^5$ °C m^{-1}, between LB and P1 (upper panel), and East-West velocity component (lower panel), from Dec 16, 2011, to Mar 22, 2012. Positive velocity (green to red colors) is to the east.

and upwelling by the westerly wind must increase the surface [chl-a] at LB. The delay between the front dissipation start and the high [chl-a] peaks (Figs. 5a and 7) was larger in the transition to anticyclonic circulation events. In tidally controlled seas, the delay has been related to the time used for the arrival of nutrients from their source, and the number of available chl-a cells ready to use those nutrients (Mann and Lazier, 1991).

3.5 The mechanisms of mixing.

The two smallest high [chl-a] events occurred early in the time series: Dec 18, 2011, and Jan 10, 2012, under cyclonic and anticyclonic circulation, each. The three largest high [chl-a] events occurred on Jan 19-27, Jan 31-Feb 6, and Mar 3, 2012, in cyclonic, cyclonic, and anticyclonic circulation, respectively.

On December 18, anticyclonic circulation practically occupied the area near LB (Figure 8a). Wind was westerly and moderate over the west coast, but northerly and strong over the gulf (Figure 8b), forming a thermal front in north-south orientation (Figure 7 upper panel). The sea level, as given by the adt, however, was depressed (Figure 3a), consistent with a barely discernible cyclonic circulation near LB. There, the relative vorticity was negative and the Ekman pumping velocity, W_E, estimated from the ASCAT wind stress rotational, downwards (Figure 8c). The brief and modest high [chl-a] (Figure 5a), occurred under wind stress ~0.3 Nm^{-2} at MS, downward Ekman pumping velocity, W_E (from ASCAT wind), and positive relative vorticity (Figure 8c). A mixing mechanism is interpreted from the T_{w5} drop and T_{w24} increase about 1.5°C and 0.8°C respectively, from December 17 to 18 (Figure 3d). Complete mixing was reached on Dec 19. After December 18, the northerly wind over the gulf weakened, and relatively high SST water moved eastward, while at depth, water moved westward (Figure 7), increasing stratification towards Dec 21.

On Jan 10, an anticyclonic circulation occupied the West Coast, and a cyclonic circulation the GT (Figure 9a). Weak westerly wind occupied both the west coast and the WMGT (Figure 9b). The sea level, as given by the adt (Figure 3a), although relatively high, was descending, in consistency with the southwestward retrieval of the anticyclone. Despite this circulation, in the area next to LB, the relative vorticity was positive and W_E was downwards (Figure 9c).

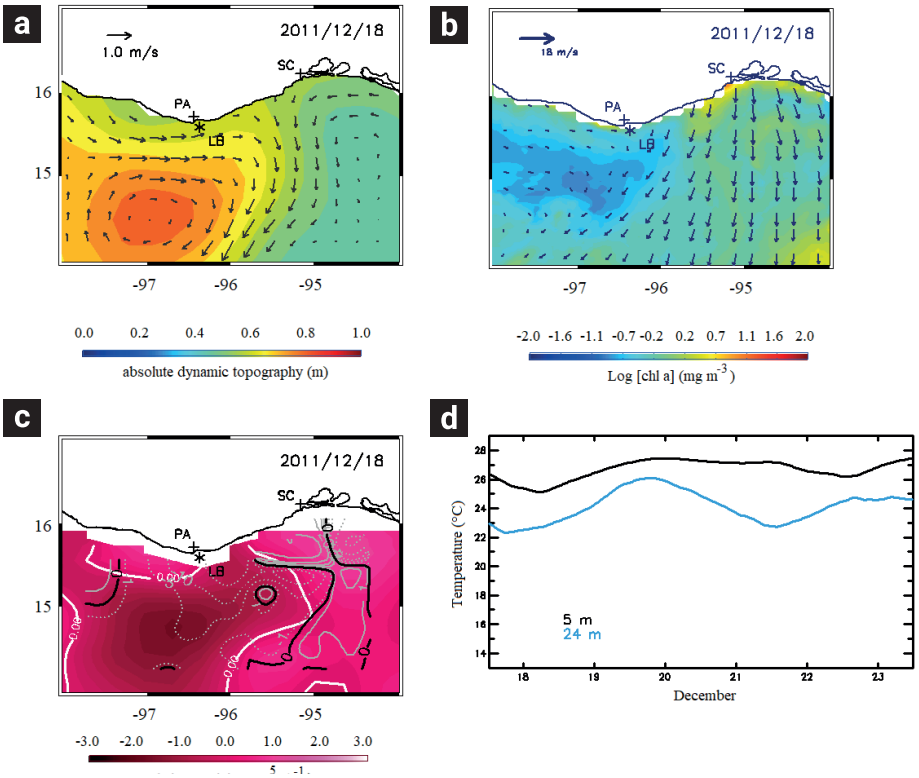

Figure 8. Panels a) Absolute dynamic topography (adt) and geostrophic current vectors; b) Chlorophyll-a concentration and wind velocity vectors; c) Estimated Ekman vertical velocity $W_E \times 10^6$ (grey and black lines) and relative vorticity $\times 10^5$ (colors and white line); d) T_{w5} and T_{w24} recorded in the mooring site from Dec 17 to 23, 2011. a) and b) correspond to Dec 18, 2011. $W_E > 0$, upwards

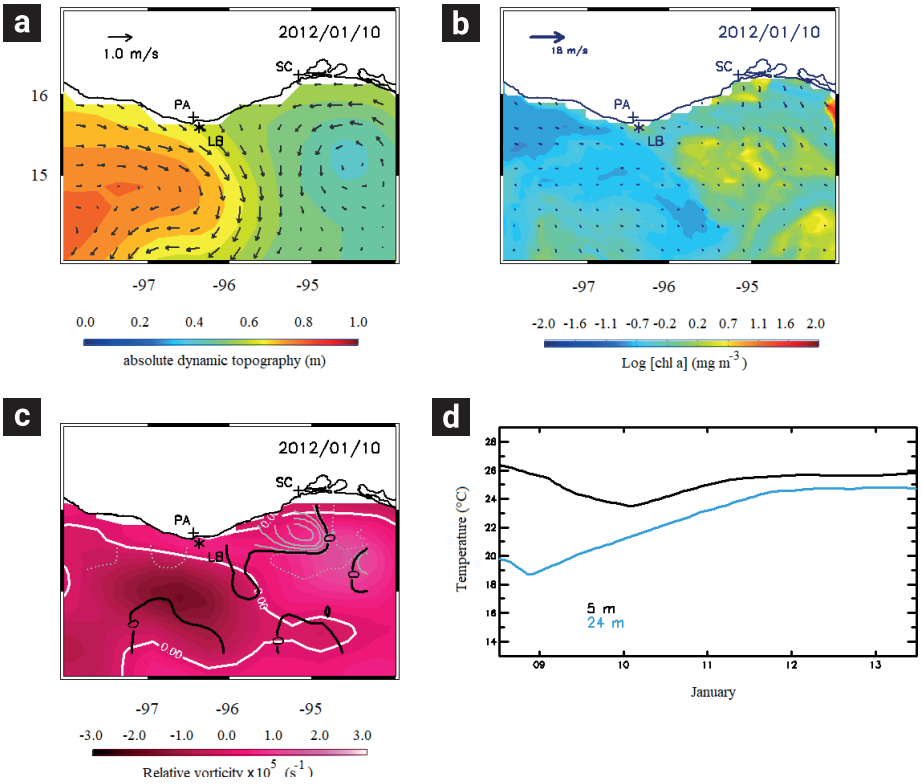

Figure 9. Panels a) Absolute dynamic topography (adt) and geostrophic current vectors; b) Chlorophyll-a concentration and wind velocity vectors; c) Estimated Ekman vertical velocity $W_E \times 10^6$ (grey and black lines) and relative vorticity $\times 10^5$ (colors and white line); d) T_{w5} and T_{w24} recorded in the mooring site from Jan 8 to 13, 2012. a) and b) correspond to Jan 10, 2012. $W_E > 0$, upwards.

The high [chl-a] occurred under westerly wind stress about 0.3 Nm^{-2} at the MS (Figure 5a), preceded by the dissipation of a north-south oriented thermal front in the gulf (not shown), and strong stratification on Jan 8 (Figure 5b). Mixing conditions are indicated by the ~2.7°C, T_{w5} descent, and 3.3°C, T_{w24} ascent from Jan 8 to 10 (Figure 9d). The increase in T_{w5}, posterior to Jan 10, in despite of the mixing with T_{w24}, can be explained by the eastward spread of relatively high SST water following the thermal front dissipation (Figure 7). The [chl-a] dropped below its average value (Fig 5a) as the water column reached complete mixing on Jan 12.

The high [chl-a] event from Jan 19 to 27 consisted of two moments, the first moment starting days before the event: From Jan 15 to 24, an anticyclone moved southwestward from its most northern position, with its northeast edge to the west of LB and cyclonic circulation in the GT (not shown). From Jan 25 to 27, the anticyclone kept southwest, relatively distant from LB, and the cyclone in the GT remained without major changes. The position of the anticyclone varied accordingly with the wind conditions: From Jan 15 to 19, northerly wind occupied the GT, and moderate westerly wind the West Coast. From Jan 20 to 24, westerly wind dominated over the West Coast and the GT. From Jan 25 to beyond Jan 27, modest and variable winds occupied the West Coast, and northerly winds occupied the GT. Figures 10a and 10b present the conditions on Jan 21, with the anticyclone to the southwest of LB, and westerly wind over the West Coast and GT.

In terms of the SST, from Jan 15 to 19, with northerly wind on the GT, a thermal front moved westward to reach and surpass the LB mooring, such that on Jan 20 the horizontal temperature gradient disappeared (Figure 7, upper panel). From Jan 20 to 25, under westerly wind, the sign of the temperature gradient was inverted as a warm surface plume filled the GT from the east following the geostrophic cyclonic circulation (not shown); consequently, the SST at LB was lower than at the central gulf. From Jan 26 to 27, the warm surface water from the GT reached LB, and the inverted temperature gradient was dissolved. In the area next to LB, the sea level as given by the adt reached a minimum (Figure 3a), consistently with the positive relative vorticity close to LB; and W_E was upwards (Figure 10c).

The [chl-a] reached values above its mean for westerly wind stress above 0.4 Nm^{-2} at the MS (Figure 5a). From Jan 17 to 21, T_{w5} fell for about 3.9°C, to reach T_{w24}, which remained relatively unchanged (Figure 10d); this fact is interpreted as upwelling. On Jan 24, the westerly wind started to weaken and stratification increased; at LB, the [chl-a] diminished but remained above its mean. From Jan 26 to 27, the northerly wind returned to the WMGT, and mixing at LB pointed to the termination of the high [chl-a] event.

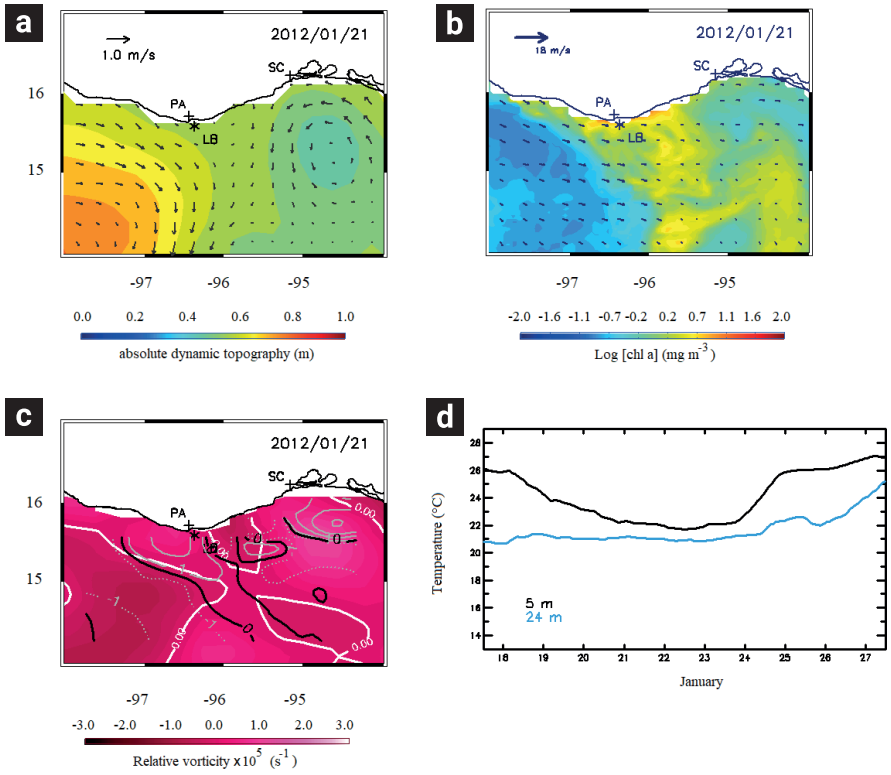

Figure 10. Panels a) Absolute dynamic topography (adt) and geostrophic current vectors; b) Chlorophyll-a concentration and wind velocity vectors; c) Estimated Ekman vertical velocity $W_E \times 10^6$ (grey and black lines) and relative vorticity $\times 10^5$ (colors and white line); d) T_{w5} and T_{w24} recorded in the mooring site from Jan 17 to 27, 2012. a) and b) correspond to Jan 21, 2012. $W_E > 0$, upwards.

From Jan 31 to Feb 6, an anticyclone progressively approached LB from the south; in correspondence, cyclonic circulation in the GT moved eastward. Although variable in speed, strong northerly wind was dominant on the GT, while over the west coast, westerly wind was mostly weak. Figures 11a and 11b show the conditions present on Feb 2. From Jan 30 to 31, a thermal front crossing through the LB mooring (not shown), moved westward, and consequently the horizontal temperature gradient between LB and P1 decreased (Figure 7). From Feb 2 to 6 however, to the southeast of LB, a warm surface water arm protruded from the warm water pool towards the WMGT following and anticyclonic path (not shown), increasing the estimated temperature gradient from Feb 4 to 6. Near to LB however, both, the relative vorticity and W_E were barely positive (Figure 11c). The [chl-a] was above its mean value (Fig 5a), but this did not occur after the transition from northerly to the westerly wind in the WMGT, but under strong northerly wind in the GT; at the MS, $\tau < 0.02$ N m^{-2} (Fig 5c). Weak stratification existed through most of the period, with an overall temperature descent at both depths, $T_{w5} \sim 2$°C and $T_{w24} \sim 1$°C (Figure 11d). The descent on T_{w5} is interpreted due to a relatively light and shallow mixing layer; on the other hand, that of T_{w24} is due to the permanent arrival of cool subsurface water.

On Mar 3, the high [chl-a] was the highest of the five identified events (Figure 5a). It was preceded by a relatively long period of strong stratification (Figure 5b), after northerly wind weakening and thermal front dissipation from Feb 26 to Mar 1 (Figure 7 upper panel). Despite the decaying northerly wind, from Feb 26 to beyond Mar 3, anticyclonic circulation occupied the West Coast and the GT border (see, for example, Figure 3a), and cyclonic circulation the eastern gulf. Winds were northerly on the GT and weak and westerly on the West Coast, from Feb 26 to 29. From Mar 1 to 2, intense westerly winds occupied both the West Coast and the GT, but on Mar 3, northerly winds occupied both regions. Correspondingly, high [chl-a] extended progressively along the coast from the central gulf to the WMGT. Figures 12a and 12b show the conditions present on Mar 2. At LB, the relative vorticity and W_E were positive and negative, respectively (Figure 12c). The high [chl-a] occurred for westerly wind stress at the MS > 0.04 Nm^{-2}. T_{w5} decreased for about 4.9°C, to practically reach T_{w24}, which remained reasonably unchanged, suggesting a process of upwelling and mixing (Figure 12d).

4. Discussion and conclusions

Five events with daily high [chl-a], above its temporal mean, 2.3 mg m^{-3}, from Dec 2011 to Mar 2012, were analyzed in the

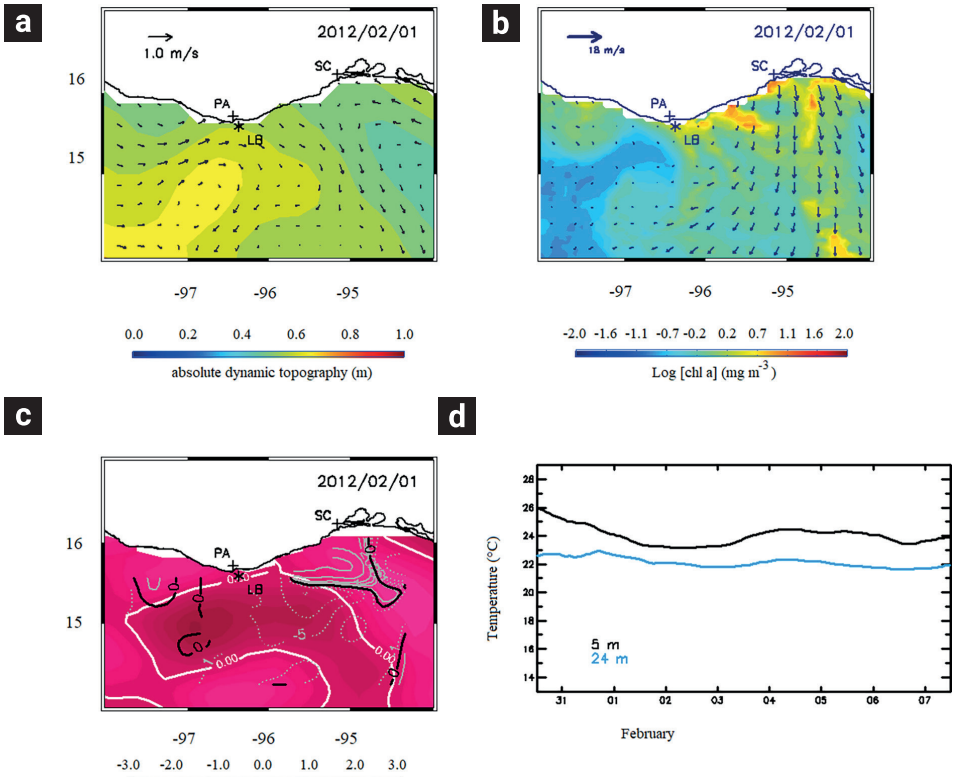

Figure 11. Panels a) Absolute dynamic topography (adt) and geostrophic current vectors; b) Chlorophyll-a concentration and wind velocity vectors; c) Estimated Ekman vertical velocity $W_E \times 10^6$ (grey and black lines) and relative vorticity $\times 10^5$ (colors and white line); d) T_{w5} and T_{w24} recorded in the mooring site from Jan 30 to Feb 7, 2012. a) and b) correspond to Feb 1, 2012. $W_E > 0$, upwards.

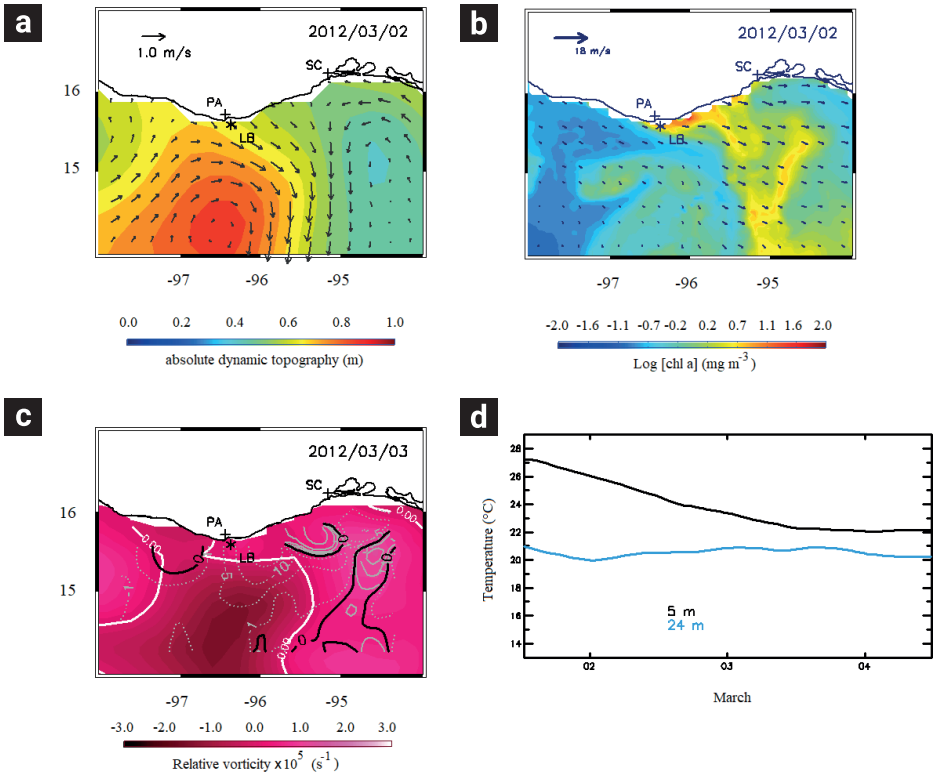

Figure 12. Panels a) Absolute dynamic topography (adt) and geostrophic current vectors; b) Chlorophyll-a concentration and wind velocity vectors; c) Estimated Ekman vertical velocity $W_E \times 10^6$ (grey and black lines) and relative vorticity $\times 10^5$ (colors and white line); d) T_{w5} and T_{w24} recorded in the mooring site from Mar 1 to 4, 2012. a) and b) correspond to Mar 2, 2012. $W_E > 0$, upwards.

context of stratification, wind, and mesoscale circulation at LB, a point between the West Coast and the WMGT.

During the period of observations, the West Coast and the WMGT were occupied by anticyclonic and cyclonic circulation features, respectively. Generally under northerly wind, an anticyclone approached LB, and a cyclone in the central GT, and under westerly wind, the anticyclone was located southwestward of LB, and the cyclone occupied the WMGT.

In general, the high [chl-a] events occurred during weak or absent stratification ($\Delta T \leq 1.3$ °C), which is a function of the wind and the mesoscale circulation next to LB (Reyes-Hernández and Ahumada-Sempoal, 2022). These events occurred mainly under strong westerly winds ($\tau \geq 0.04$ Nm^{-2}) and thermal front dissipation (Jan 10, Jan 19-27, and Mar 3), but also under weak (Dec 18; $\tau \leq 0.04$ Nm^{-2}) or even negligible (Jan 31-Feb 6) westerly wind on the West Coast, but strong northerly wind on the GT and thermal front formation. The highest and lasting high [chl-a] events (4-18 mg m^{-3}) on Jan 19-27, and Jan 31-Feb 6, corresponded with cyclonic circulation approaching LB or also anticyclonic circulation relatively separated from LB; the smallest high [chl-a] events, on Dec 18 and Jan 10, occurred for cyclonic or anticyclonic circulation next to LB respectively, On the other hand, the conditions of [chl-a] below the mean value clearly occurred under anticyclonic circulation next to LB (Figs. 3a and 5a). A particular condition was the highest [chl-a] event, on Mar 3, which occurred with the strongest westerly wind from the whole period of observation and anticyclonic circulation next to LB.

Northerly wind on the GT forms a thermal front between the GT and the West Coast, mainly oriented in a north-south direction (Figure 6). Under strong northerly wind on the GT, the front may be located to the west of LB, and under moderate or no northerly wind at all, to the east of LB. Consistently, with the front, a horizontal temperature gradient sets up between LB and the central GT.

Anticyclonic and cyclonic mesoscale circulations depress and elevate the thermocline, respectively; however, as the mesoscale circulation approached LB, a counter-circulation formed between LB and the coast, apparently as a result of lateral velocity shear in the eastward current along the West Coast, and in the southward current along the WMGT coast. This effect seems to provide an additional thermocline depth modification in addition to that produced by the mesoscale circulation.

Each of the two anticyclonic features that approached LB, derived from a correspondent anticyclonic eddy centered around 14°N and 96.5°W. The first eddy formed from a northerly wind

event on the GT on Dec 2, 2011; the second one originated on Jan 30, 2012, under strong westerly winds. Each anticyclonic circulation approached LB as an elongated deformation from the northern edge of the respective parent eddy. From Dec 30 to Jan 7, the anticyclonic circulation oriented nearly parallel to the West Coast, with eastward geostrophic velocities reaching LB from the west (not shown). Moderate westerly winds initiated on Jan 7 (Figure 5a), and a relatively quick adt sea level drop followed (Figure 3a). From Feb 12 to Mar 9, the anticyclonic elongation oriented meridional (see, for example, Figure 12a); therefore, the geostrophic velocities were northward, against the coast, contributing to the rise and permanence of the high adt near to LB. This anticyclonic circulation remained close to LB in despite of the strong westerly winds blowing from Feb 12 to 19 (Figure 5a). The southwestward drift of the anticyclonic circulation under weak westerly wind, in the first case, and its permanence near the coast under strong westerly wind, in the second one, are responses similar to those discussed by Barton *et al.* (1993). They noticed that short successive northerly wind events do not allow anticyclonic eddies to migrate far from the coast; instead, each wind event reinforces them. However, if the northerly wind events occur sufficiently spaced, anticyclonic eddies migrate offshore far enough, such that a following wind event will spin up a new eddy.

For a relatively deep thermocline corresponding to an anticyclonic circulation, it is possible that W_E cannot provide the necessary conditions for chlorophyll-a to flourish, keeping its concentration low. In this sense it is illustrative to compare the low [chl-a] conditions on Feb 12 to 19, to those high [chl-a] events on Jan 19 to 27, and on Jan 31 to Feb 6 (Figure 5a). Feb 12 to 19 and Jan 19 to 27, had similar strong westerly wind conditions ($\tau > 0.04$ Nm^{-2}, Figure 2c), in contrast, on Jan 31 to Feb 6, the West Coast was occupied by negligible wind, but strong northerly wind in the GT.

From Feb 12 to 19, a northeastward elongated anticyclonic circulation occupied the WMGT and cyclonic circulation the eastern GT. The northerly wind relaxation over the gulf led to the thermal front dissipation between the WMGT and the central gulf (not shown), producing a strong estuarine-type circulation (Figure 7, lower panel). The westerly wind stress at MS did not lead to mixing but to the strongest stratification that occurred in the whole period (Figure 5a). A possible explanation for this is that the westerly wind fed up momentum to the surface anticyclonic circulation, depressing the thermocline, plunging the subsurface layer, and consequently keeping the [chl-a] low.

From Jan 19 to 27, the northern edge of anticyclonic circulation also occupied the West Coast and cyclonic circulation the GT, while westerly wind occupied both coasts. In comparison to Feb 12-19, both the anticyclone and cyclone are located further westward. In the GT, the westerly wind and the cyclonic circulation lead to the cyclonic twist of the thermal front, which moved west of LB (not shown), weakening the E-W two-layer flow (Figure 7, lower panel). The anticyclonic circulation relatively far from LB and the westerly wind on the West Coast were favorable for coastal upwelling, as it is indicated by the high [chl-a] stretching from the West Coast into the GT (Figure 10b). The evolution of stratification at LB (Figure 10d) is indicative of upwelling.

From Jan 31 to Feb 6, the West Coast experienced an anticyclonic circulation approaching LB, similar to that of Feb 12 to 19, and negligible wind (Figs. 3a and 5a). In the GT, however, northerly wind was strong, forming a thermal front to the west of LB, and the cyclonic circulation drifted eastward (Figure 3a). The northerly wind speed and thermal front weakened from Jan 30 to Feb 3 (Reyes-Hernández and Ahumada-Sempoal, 2022; their Figure 2b), producing an anticyclonic motion of surface warm water (not shown). An E-W two-layer flow occurred between 12 and 24 m depth from Jan 31 to Feb 2, and between 4 and 6 m depth from Feb 3 to Feb 6 (Figure 7 lower panel). The high [chl-a] reached under weak and shallow wind mixing energy at LB (Figure 11b), pointing towards the near-surface availability of chl-a and nutrients by the two-layer exchange.

In the very simple assumption that the high [chl-a] depended only on the depth of nutrients transport by the subsurface water and no other factors, such as the light availability; the [chl-a] peaks on Jan 19-27, Jan 31-Feb 6 (strong westerly winds and cyclonic circulation), and Mar 3 (very strong winds and anticyclonic circulation), had better nutrients availability conditions than those on Dec 18 (modest winds and cyclonic circulation) and Jan 10 (modest winds and anticyclonic circulation).

Although we did not perform any light transmission in water observation, we conjecture that the occurrence of the high [chl-a] in anticipation of complete vertical mixing in the water column is related to the transparency of the water. The high [chl-a] is reached when the optimum amount of available light and nutrients is met. Under complete mixing, turbidity reduces the light availability and consequently the ability for photosynthesis, even if there is availability of nutrients. Some degree of stratification should guarantee enough water transparency (Mann and Lazier, 1991).

6. Acknowledgments

NOA-ESRL SLP image. Support for the Twentieth Century Reanalysis Project dataset is provided by the U.S. Department of Energy, Office of Science, Innovative and Novel Computational Impact on Theory and Experiment (DOE INCITE) program, and Office of Biological and Environmental Research (BER),

and by the National Oceanic and Atmospheric Administration Climate Program Office.

The fieldwork was partially funded by the now National Council for Humanities, Science, and Technology (CONAHCYT) through the project Basic Science 80228 and through the regular budget of Universidad del Mar. Thanks go to Ocean. Ángel Cuevas, Tech. Sergio Vázquez Mendoza and the UMAR-I crew: Eladio Espíndola, Andrés Pacheco and Leonídes Aquino.

5. References

Almaraz-Ruiz (2013). Variación temporal de la comunidad de diatomeas en el noroeste del Golfo de Tehuantepec durante los meses de febrero a julio del 2006. [Tesis de Licenciatura], Universidad del Mar.

Barton, E. D., Argote, M. L., Brown, J., Kosro, P. M., Lavín, M., Robles, J. M., Smith, R. L., Trasviña, A., and Vélez H. S. (1993). Supersquirt: Dynamics of the Gulf of Tehuantepec, México. *Oceanography*, 6(1), 23-30. doi: **https://doi.org/10.5670/oceanog.1993.19**

Blackburn, M. (1962). *An oceanographic study of the Tehuantepec. U. S. Fish and Wildlife Service* (Special Scientific Report No. 404). United States Fish and Wildlife Service.

Carr, M.-E., & Kearns, E. J. (2003). Production regimes in four Eastern Boundary Current systems. *Deep Sea Research Part II: Topical Studies in Oceanography*, *50*(22–26), 3199–3221. doi: **https://doi.org/10.1016/j.dsr2.2003.07.015**

Cervantes-Hernández, P., Sánchez-Meraz, B., Serrano-Guzmán, S. J., Frías-Velasco, A., Ramos-Cruz, S. y Gracia, A. (2008). Variación interanual de la abundancia de Farfantepenaeus californiensis (Holmes, 1900) en el Golfo de Tehuantepec. Hidrobiológica 18(3), 215-226. **https://hidrobiologica.izt.uam.mx/index.php/revHidro/article/view/903**

Chapa-Balcorta, C., Hernandez-Ayon, J. M., Durazo, R., Beier, E., Alin, S. R., & López-Pérez, A. (2015). Influence of post-Tehuano oceanographic processes in the dynamics of the CO2 system in the Gulf of Tehuantepec, Mexico. *Journal of Geophysical Research: Oceans*, *120*(12), 7752–7770. doi: **https://doi.org/10.1002/2015JC011249**

Gaxiola-Castro, J., Cepeda-Morales, S., Nájera Martínez, T. L., Espinoza-Carreón, M., de la Cruz-Orozco, E., Sosa-Avalos, R., Aguirre-Hernández, E. & Cantú-Ontiveros, J. P. (2010). Biomasa y producción del fitoplancton. En A. Gilberto Gaxiola-Castro y Reginaldo Durazo (Eds.). *Dinámica del ecosistema pelágico frente a Baja California 1997-2007* (pp. 59-86). Secretaría del Medio Ambiente y Recursos Naturales (Semarnat); Instituto Nacional de Ecología (INE); I Centro de Investigación Científica y de Educación Superior de Ensenada (CICESE); Universidad Autónoma de Baja California (UABC).

Large, W. G., & Pond, S. (1981). Open Ocean Momentum Flux Measurements in Moderate to Strong Winds. *Journal of Physical Oceanography*, *11*(3), 324–336. **https://doi.org/10.1175/1520-0485(1981)011%3C0324:OOMFMI%3E2.0.CO;2**

Lluch-Cota, S., Álvarez-Borrego, S., Santamaría-Ángel, E., Müller-Karger, F., & Hernández-Vázquez, S. (1997). The Gulf of Tehuantepec and adjacent areas: spatial and temporal variation of satellite-derived photosynthetic pigments. *Ciencias Marinas*, *23*(3), 329–340. doi: **https://doi.org/10.7773/cm.v23i3.809**

Mann, K. H., & Lazier, J. R. N. (1991). *Dynamics of marine ecosystems: biological-physical interactions in the oceans*. Blackwell Scientific Publications.

Niiler, P. P., and Kraus, E. B. (1977). One-dimensional models of the upper ocean. In E. B. Kraus (Ed.), *Modelling and Prediction of the upper layers of the ocean*. (pp. 143-172). Pergamon Press.

Pennington, J. T., Mahoney, K. L., Kuwahara, V. S., Kolber, D. D., Calienes, R., & Chavez, F. P. (2006). Primary production in the eastern tropical Pacific: A review. *Progress in Oceanography*, *69*(2–4), 285–317. doi: **https://doi.org/10.1016/j.pocean.2006.03.012**

Portela, E., Beier, E., Barton, E. D., Castro, R., Godínez, V., Palacios-Hernández, E., Fiedler, P. C., Sánchez-Velasco, L., & Trasviña, A. (2016). Water Masses and Circulation in the Tropical Pacific off Central Mexico and Surrounding Areas. *Journal of Physical Oceanography*, *46*(10), 3069–3081. doi: **https://doi.org/10.1175/JPO-D-16-0068.1**

Reyes-Hernández, A. C., & Ahumada-Sempoal, M. A. (2022). Coastal stratification and mixing on the western margin of the Gulf of Tehuantepec within a synoptic atmospheric and oceanographic environment. *Continental Shelf Research*, *246*, 104810. **https://doi.org/10.1016/j.csr.2022.104810**

Reyes-Hernández, A. C., Ahumada-Sempoal, M. A., López-Pérez, A., & Malagón-Pimentel, X. (2019). Surface and advective heat fluxes in the western margin of the Gulf of Tehuantepec. *Continental Shelf Research*, *180*, 35–47. doi: **https://doi.org/10.1016/j.csr.2019.04.011**

Reyes-Hernández, C., Ahumada-Sempoal, M. Á., & Durazo, R. (2016). The Costa Rica Coastal Current, eddies and wind forcing in the Gulf of Tehuantepec, Southern Mexican Pacific. *Continental Shelf Research*, *114*, 1–15. doi: **https://doi.org/10.1016/j.csr.2015.12.012**

Trasviña, A. and Barton, E. D. (1997). Los 'Nortes' del Golfo de Tehuantepec: La circulación costera inducida por el viento. En A. M. Lavin (Ed.) *Contribuciones a la Oceanografía Física en México. Monografía No. 3*, Unión Geofísica Mexicana.

Trasviña, A., Barton, E. D., Brown, J., Velez, H. S., Kosro, P. M., & Smith, R. L. (1995). Offshore wind forcing in the Gulf of Tehuantepec, Mexico: The asymmetric circulation. *Journal of Geophysical Research: Oceans*, *100*(C10), 20649–20663. doi: **https://doi.org/10.1029/95JC01283**

Willett, C. S., Leben, R. R., & Lavín, M. F. (2006). Eddies and Tropical Instability Waves in the eastern tropical Pacific: A review. *Progress in Oceanography*, *69*(2–4), 218–238. doi: **https://doi.org/10.1016/j.pocean.2006.03.010**

Zamudio, L., Hurlburt, H. E., Metzger, E. J., Morey, S. L., O'Brien, J. J., Tilburg, C., & Zavala-Hidalgo, J. (2006). Interannual variability of Tehuantepec eddies. Journal of Geophysical Research: Oceans, 111(C5), 2005JC003182. doi: **https://doi.org/10.1029/2005JC003182**